PSFC/JA-11-30

Co- and Counter-current Rotation Induced by Lower Hybrid Current Drive in Tokamak Plasmas

Podpaly, Y.A., Rice, J. E., Parker, R. R., Reinke, M. L., Shiraiwa, S., Delgado-Aparicio, L.*, Scott, S.*, Ennever, P., Gao, C., Irby, J., Lee, J. P., Meneghini, O., Mumgaard, R., Porkolab, M., Tsujii, N., Walk, J. R., and Wallace, G.

* Princeton Plasma Physics Laboratory

December, 2011

Plasma Science and Fusion Center
Massachusetts Institute of Technology
Cambridge MA 02139 USA

Co- and Counter-current Rotation Induced by Lower Hybrid Current Drive in Tokamak Plasmas

Y. A. Podpaly,[1] J. E. Rice,[1] R. R. Parker,[1] M. L. Reinke,[1] S. Shiraiwa,[1] L. Delgado-Aparicio,[2] S. Scott,[2] P. Ennever,[1] C. Gao,[1] J. Irby,[1] J. P. Lee,[1] O. Meneghini,[1] R. Mumgaard,[1] M. Porkolab,[1] N. Tsujii,[1] J. R. Walk,[1] and G. Wallace[1]

[1]*MIT Plasma Science and Fusion Center, Cambridge, MA 02139*
[2]*Princeton Plasma Physics Laboratory, Princeton, NJ 08540*
(Dated: November 10, 2011)

Lower Hybrid Current Drive induced rotation changes in both the co- and counter-current direction have been observed in Alcator C-Mod L-mode plasmas. At fixed density, the induced rotation is in the counter-current direction at high plasma currents, but, at a critical current, it reverses direction to the co-current direction. Below the critical current, the plasma rotation scales inversely with plasma current. For $<n_e> = 0.66 \times 10^{20} \mathrm{m}^{-3}$, the critical current appears to depend on magnetic configuration with the reversal occurring at ~ 550 kA in unfavorable ∇B drift direction and ~ 400 kA in favorable ∇B drift direction.

Recently, plasma rotation generation in tokamaks has been an area of active interest due to the effect of rotation in suppressing resistive wall modes and in modifying transport. This research has also focused on finding rotation drive other than through tangential neutral beam injection since neutral beams will be severely limited on reactor size tokamaks due to high densities and large reactor dimensions. Another area of active research has focused on the generation of non-inductive current drive, in order to sustain extended plasma confinement beyond the limits of the central transformer. One of the major mechanisms of sustaining this plasma current has been Lower Hybrid Current Drive (LHCD), which has been found to be fairly efficient and is one of the systems under consideration for ITER [1].

LHCD has previously been seen to induce rotation in Alcator C-Mod plasmas [2, 3]. This rotation was observed to be in the counter-current direction and scales with P_{LH}/n_e. Furthermore, the rotation magnitude is proportional to the internal inductance, l_i, which can be considered a proxy for the current profile modification. The rotation was also seen to scale inversely with the parallel refractive index, $n_{||} = ck_{||}/\omega$, which controls the location of the fast electron distribution on which the wave damps its power.

LHCD induced rotation had also been observed at JT-60U [4], Tore Supra [5], JET [6], and, recently, at EAST [7]. In all of these cases, the rotation was in the co-current direction, with JT-60U reporting that the entire profile was elevated. It was proposed that this co-current rotation was due to ripple losses of fast electrons or an inward turbulent equipartition pinch from the edge of the plasma.

Recently, co-current LHCD induced rotation was observed for the first time at Alcator C-Mod. This was seen in both upper single null (USN, unfavorable $B \times \nabla B$ drift direction) discharges and in lower single null (LSN, favorable $B \times \nabla B$ drift direction). The experiment was performed on Alcator C-Mod [8] at $B_T = 5.4$T, $<n_e> = 0.66 \times 10^{20} \mathrm{m}^{-3}$, plasma elongation $\kappa \approx 1.6$, and no auxiliary heating other than that due to LH wave injection. Plasma current at the target density was scanned from 300 kA through 900 kA. The lower hybrid launcher was run at 800 kW of net power into the plasma and at a launched refractive index of 1.6, which is known to give a large counter-current rotation from the previous LHCD rotation results.

These plasmas had argon impurity puffing for use with the imaging x-ray spectrometer [9], which provided all of the rotation profiles shown in this work. Rotation calibration was accomplished by running a locked mode discharge which brakes the rotation to find $v_\phi(r) = 0$. Positive rotation direction in these results is always in the direction of the current. Averaged plasma density values are from a two color interferometer. Throughout the experiment, plasma density and net forward power from the LH launcher were repeatable to within 20%.

Overall, several reproducible discharges were accomplished in upper single null and lower single null. A fairly characteristic trace of the plasma rotation in both the co- and counter-current directions is shown in figure 1. During the high current case (black trace), the rotation drive was in the counter-current direction with a rotation change of ~ 30 km/s. At low current (green trace), however, the core rotation is driven in the co-current direction $\Delta v \sim 30$ km/s and only appears to initiate after ~ 100 ms of the LHCD pulse at comparable densities. All of the upper single null discharges were sawtooth stabilized by LHCD, with the time of the stabilization depending on the current. The high current lower single null discharges had sawteeth all throughout the discharge, while the sawteeth were stabilized in the lower current cases. It is interesting to note that after the LHCD system turned off, there were differences in how the rotation trace recovered to its pre-LHCD phase value. The high current case relaxes to its pre-LHCD value on a current relaxation time scale (~ 100 ms), while the low current case returned to its pre-LHCD rotation value on

a momentum confinement time scale(~ 20 ms). This relaxation mechanism is not understood and may shed light on why the original rotation changes are different as well, but this has not currently been analyzed.

The summary of the rotation results for different currents is shown in figure 2. The change in core rotation is calculated by subtracting the pre-LHCD rotation from the final rotation during the LHCD phase. It is observed that the plasma current has a very strong effect on the plasma rotation magnitude and rotation direction. Furthermore, the USN and LSN plasmas show a marked difference in the rotation behavior. The critical rotation zero-points for the USN and LSN plasmas are approximately 550 kA and 400 kA, respectively.

FIG. 2: Rotation change due to LHCD versus plasma current. Diamonds (asterisks) represent equilibria with ion ∇B drift towards (away from) the x-point. Red points are from 2008 data; density and LHCD power are 10% higher than current values, and the points are shown for comparison to highlight why this effect has not been observed previously. All data from respective years are at fixed density and power. The dashed red line marks the theoretical position of the intrinsic plasma rotation reversal.
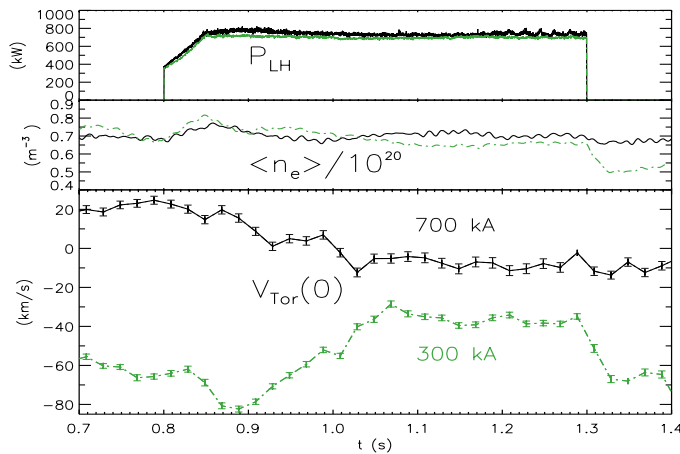

FIG. 1: Characteristic time histories (taken in the USN case) of LHCD induced rotation: lower hybrid power, averaged density, and core rotation, are shown. Dashed, green lines represent the 300 kA case with co-current rotation and black lines represent the 700 kA case with counter-current rotation. Statistical error bars are shown on the rotation traces.

FIG. 3: Characteristic rotation profiles at various times during the discharge for two USN discharges. Both high and low current cases are shown, and statistical errors bars are shown as well.

Rotation profiles of the USN and LSN cases at high and low current are shown in figures 3 and 4. It is observed that the rotation profiles appear to be pinned at r/a $\approx$ 0.5-0.6, which suggests that the effect of the LHCD rotation drive is more localized to the core of the plasma than to the edge. As seen in the figures 3 and 4, at the start of LHCD, the rotation at high currents transitions to the counter current direction, while low current discharges have co-current rotation profiles with the largest change located in the core.

It has been proposed that the counter-current direction of rotation is caused by the direct momentum input of the waves driving fast electrons in the counter-current direction [10]. The electrons then collisionally couple to the main ion species and drive counter current directed momentum. The estimated rotation drive, using this method, can be approximated with $n_i m_i \Delta(R v_\phi)/\Delta t = T_{LH} = R n_{||} P_{LH}/c$ and leads to a ~ 40 km/s change from LHCD, which is the correct order of magnitude in the counter current direction. This calculation assumes a
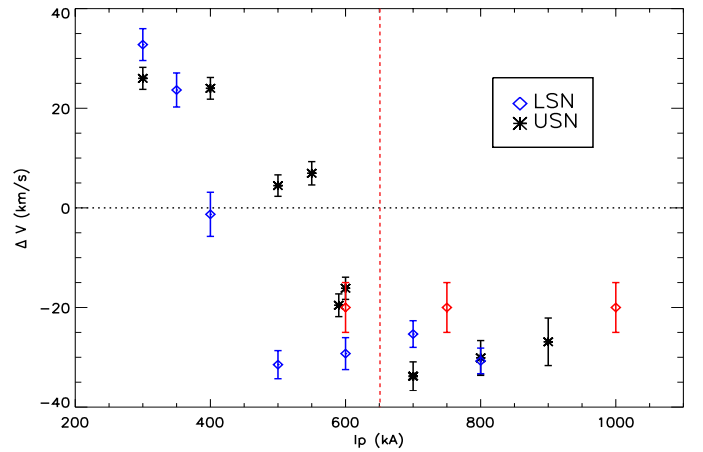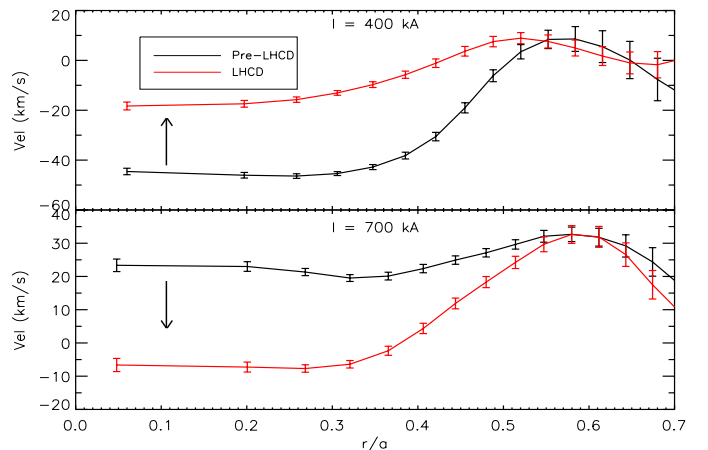
time constant of the change of ~ 100 ms, which is what is normally measured on Alcator C-Mod and is also approximately the current relaxation time. While this method may explain the counter-current rotation observed previously and produces synthetic rotation profiles that qualitatively agree with the experiment, it does not explain how LHCD can drive co-current rotation. There have been a number of proposals about what could be the reason for this co-current rotation; two methods of note are fast electron losses at the edge of the plasma and intrinsic rotation changes.
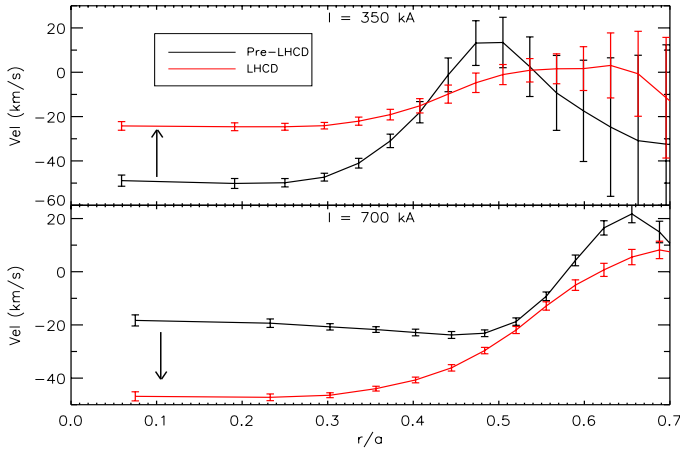
FIG. 4: Characteristic rotation profiles at various times for two LSN discharges. Both high and low current cases are shown, and statistical errors bars are shown as well. Note that error bars in the low current case around r/a = 0.5 increase due to uncertainties in the EFIT reconstruction.

Fast electron losses were the originally suggested method from the Tore Supra and JT-60U groups and drive rotation by creating a radial electric field which causes rotation drive via radial force balance. This method, however, is considered unlikely for the Alcator C-Mod device because C-Mod's ripple field is approximately 1% [11], whereas Tore Supra's is approximately 7%. Furthermore, in work performed at Tore Supra, it was found that the loss current due to magnetic ripple increases linearly with plasma current [12], which suggests that the co-current rotation should also scale linearly with increasing plasma current, whereas it does the exact opposite at C-Mod. Along with the observation that the rotation initiates in the core rather than the edge, these findings point to a different driver for co-current rotation than ripple losses of fast electrons.

The second proposed method for LHCD rotation reversal is modification of intrinsic rotation via changes in the profiles. Ohmic L-mode plasmas have been observed to reverse rotation direction spontaneously as a function of current, density, and magnetic field [13–15], and this effect is thought to be due to turbulence changes in the plasma. The profiles of rotation remain fixed at the $q = 3/2$ surface. The observed reversal current at the operational density and magnetic field of the LHCD experiment is ≈ 650kA, which is marked in figure 2. This current is within 20% of the calculated LHCD induced reversal point based on the scaling in [15], so it suggests that there are turbulence caused changes in the plasma behavior. Furthermore, during counter-current directed rotation, there are observations of assymetric turbulence in density fluctuations using the phase contrast imaging (PCI) diagnostic, which is shown in figure 5. This turbulence does not appear in the low current plasmas in LSN. The PCI diagnostic was not available during the upper

single null plasmas.

These observations suggest that the LHCD is changing the intrinsic plasma behavior and that the rotation is due to a modification of the plasma profiles by the current drive. If the rotation is purely controlled by changes in the profiles, then it would not be expected to see any concurrence of the rotation behavior with direct momentum input from the launcher. The counter-rotation effect, however, seems to agree with the modeling, suggesting multiple coupled generating mechanisms. Furthermore, some of the co-current rotating plasmas have an initial counter-current change even in net co-current rotation cases supporting the argument that at least two drivers are acting.

Angular momentum transport is generally given in terms of the diffusion (proportional to ∇v), convection (proportional to v), and residual stress. In [16], the residual stress is calculated as

$$\Pi_r^{res} = -\rho_* \frac{L_s}{2c_s} \chi_i \left(\frac{\nabla T}{T} \right)^2 v_{th,i}^2 \qquad (1)$$

In this equation, the sound speed c_s, ion thermal diffusivity χ_i, ion thermal speed $v_{th,i}$, and normalized Larmor radius ρ_* are all positive definite, while the $L_s = R_0 q^2 / r (\partial q / \partial r)$ term is the only one that can be negative or positive due to the reversed shear that can be created by LHCD. Since rotation depends on the divergence of the residual stress, hollow temperature profiles can also cause rotation to reverse, but these were not observed in these LHCD plasmas. This implies that a q-profile change is causing bi-directional changes in the plasma rotation; more research on this topic can be found in [17]. Equation 1 is derived from the assumption that the q-profile is monotonically increasing, so it will require modification if the shear switches sign. Motional Stark Effect (MSE) measurements are available for certain times in these discharges, thus discrete q-profiles could be analyzed. During the 300 kA LSN case, a reversal in the q-profile was seen with a minimum in q seen at r/a $\approx$ 0.5, which is the same location that the rotation is seen to be pinned. Both LSN and USN cases are shown in figure 6. It is interesting to note that the q-profile change in LSN is significantly lower than that observed in USN, suggesting that there may be coupling issues with the LHCD power into the plasma and, perhaps, explaining the difference in rotation reversals that have been observed. Overall, while appearing to be a likely method of explaining the LHCD induced rotation changes, the observation of co-current rotation changes both with and without major q-profile modification makes this explanation more difficult to justify. A more detailed calculation of the residual stress with shear profile effects is required.

In general, it seems likely that the rotation mechanism for LHCD induced rotation is due to a combination of several different effects acting in concert. In order to understand what these mechanisms are, it will be important
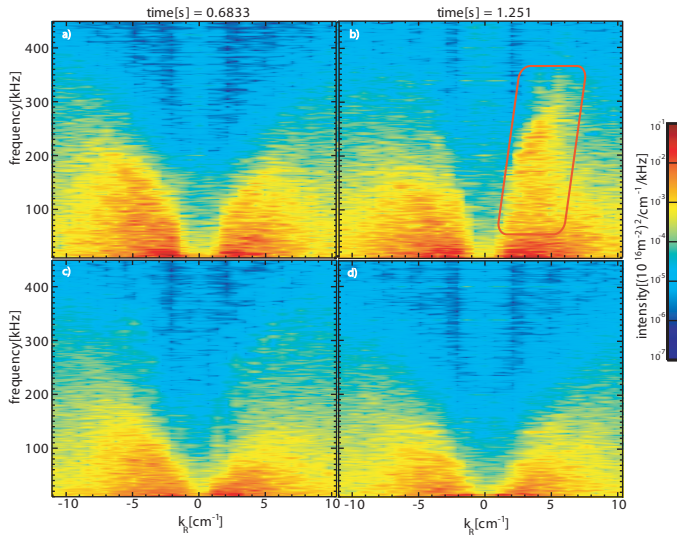
FIG. 5: PCI turbulence spectra from 700 kA(a, b) and 350 kA (c, d) discharges LSN discharges. Left columns correspond to turbulence prior to the LHCD phase and right columns correspond to turbulence ~450 ms after the turn on of the LHCD. The highlighted area shows the turbulence feature observed on the counter-current rotating LHCD plasmas.
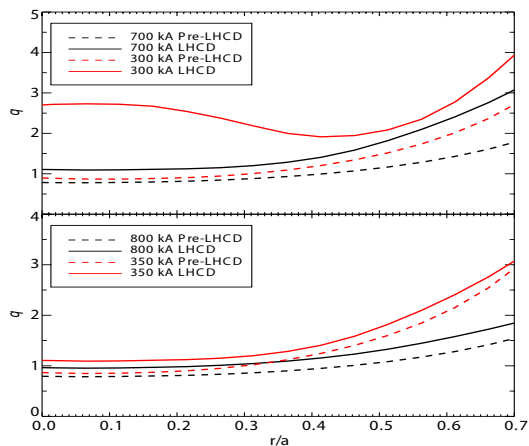

FIG. 6: Profiles of MSE constrained kinetic EFIT measurements of the q-profile. Four profiles where are shown in each plot with the top plot corresponding to USN plasmas and the bottom plot corresponding to LSN plasmas In both low current cases, reversed shears are observed.

to test whether other machines, that have only observed co-current rotation, would be able to recover counter-current rotation at high currents or observe any plasma current dependence of their rotation behavior. Another area of great interest would be confirming whether the effect is truly related to intrinsic rotation. This will be tested at Alcator C-Mod by density and magnetic field scans to identify the dependence of the LHCD induced rotation reversal point on those factors.

In summary, LHCD induced rotation has been observed for the first time in both the co- and counter-current direction in a tokamak. There is a strong plasma current dependence, and a magnetic configuration dependence appears to exist as well. Given LHCD's presence in many future tokamak designs and the importance of rotation for transport and predictability, this work helps to predict the plasma behavior in these tokamaks. It also consists of a new observation of rotation generation and could conceivably allow creating sheared rotation profiles from a single wave source improving plasma confinement.

[1] J. Decker et al., Nuclear Fusion **51**, 073025 (2011).
[2] A. Ince-Cushman et al., Phys. Rev. Lett. **102**, 035002 (2009).
[3] J. Rice et al., Nuclear Fusion **49**, 025004 (2009).
[4] Y. Koide et al., Proc. 14th Int. Conf. on Plasma Physics and Controlled Nuclear Fusion Research **1**, 777 (1993).
[5] P. Platz et al., 22nd European Physical Society Conf. on Plasma Physics and Controlled Fusion **19C** (1995).
[6] L.-G. Eriksson et al., Plasma Physics and Controlled Fusion **51**, 044008 (2009).
[7] Y. Shi et al., Phys. Rev. Lett. **106**, 235001 (2011).
[8] Alcator C-Mod Team, Fus. Sci. Tech. **51** (2007).
[9] A. Ince-Cushman et al., Review of Scientific Instruments **79**, 10E302 (2008).
[10] J. P. Lee et al., Power in Plasmas (2011).
[11] J. Irby et al., Fusion Science and Technology **51** (2007).
[12] Y. Peysson et al., Physics of Plasmas **3**, 3668 (1996).
[13] A. Bortolon et al., Phys. Rev. Lett. **97**, 235003 (2006).
[14] B. P. Duval et al., Plasma Physics and Controlled Fusion **49**, B195 (2007).
[15] J. E. Rice et al., Nucl. Fus. **In Press** (2011).
[16] J. E. Rice et al., Phys. Rev. Lett. **106**, 215001 (2011).
[17] Y. Camenen et al. Nuclear Fusion **51**, 073039 (2011).